

Multi-Robot Patrol Algorithm with Distributed Coordination and Consciousness of the Base Station's Situation Awareness

Kazuho Kobayashi¹, Seiya Ueno², and Takehiro Higuchi²

Abstract—Multi-robot patrolling is the potential application for robotic systems to survey wide areas efficiently without human burdens and mistakes. However, such systems have few examples of real-world applications due to their lack of human predictability. This paper proposes an algorithm: Local Reactive (LR) for multi-robot patrolling to satisfy both needs: (i) patrol efficiently and (ii) provide humans with better situation awareness to enhance system predictability. Each robot operating according to the proposed algorithm selects its patrol target from the local areas around the robot's current location by two requirements: (i) patrol location with greater need, (ii) report its achievements to the base station. The algorithm is distributed and coordinates the robots without centralized control by sharing their patrol achievements and degree of need to report to the base station. The proposed algorithm performed better than existing algorithms in both patrolling and the base station's situation awareness.

I. INTRODUCTION

Multi-robot patrol is a mission by multiple mobile unmanned systems to survey an assigned area for detection, reporting, and response to undesirable events or situations. Multiple robots can distribute widely in the area to survey many points simultaneously, to perform patrolling efficiently. Such systems may also enhance human safety and reduce risks of oversights and other mistakes.

On the other hand, there are few examples of the real-world applications of multi-robot systems [1]. One of the barriers is the human predictability of such systems. Since the robots work in remote areas from humans, and their internal processes and interactions with other robots are invisible, the final output of the system behavior is often unpredictable. The lack of predictability leads to concern about robot malfunctions and harmful behaviors, especially in complicated or life-threatening applications [2], [3].

A possible approach to overcome this barrier is reporting mission progress and system status frequently to the base station (BS) to provide the BS with better situation awareness (SA) [4]. In this context, the BS corresponds to the human operators or interface to them. SA may improve system predictability by enabling the BS to grasp the mission progress,

detect system malfunctions, and intervene to support decision makings.

There are various approaches for multi-robot patrol. Banfi et al. developed the SAP (Situation-Aware Patrolling) to consider both area coverage and latency of information delivery [5]. Scherer and Rinner [6] also developed an algorithm to compute both routes for patrolling and information delivery. However, such algorithms depend on the central, preliminary computation of the routes or behavior for patrol. *Distributed* and *reactive* algorithms [7] are desirable since they are robust, scalable, flexible to mission configuration, and easy to deploy. As for such algorithms, Machado et al. [8] introduced several algorithms and demonstrated that such system performs comparably to the other algorithms. Portugal et al. developed Bayesian-inspired algorithms [9], [10]. More recently, algorithms with coordination among robots by sharing their mission progress and intentions were developed [11], [12]. However, these studies have not taken the BS into account. Studies on multi-robot exploration with recurrent connectivity [13] may inspire the patrol algorithm under consideration. Though exploration missions are different from patrol missions in some aspects, the idea that recovering connections to the BS according to the mission progress can also be applied to patrol missions.

This study expands the efforts above and contributes by:

- Developing an algorithm for multi-robot patrol conscious of the base station's situation awareness
- Evaluating the performance in both patrol and base station-related perspectives

Each robot operating according to the proposed algorithm, Local Reactive (LR), selects its patrol target from the local area around the robot's current locations by two needs: patrolling and reporting to the BS. The proposed algorithm is distributed and works without instructions and coordination by the BS. The following sections describe the problem definition (Section II), proposed algorithm (Section III), simulation results (Section IV), and conclusion (Section V).

II. PROBLEM SETTINGS

This section describes the problem setting of this research. The research assumes patrol for large open areas (e.g., border areas, disaster zone, recreational sites) by unmanned aerial/surface/underwater vehicles (UAV/USV/UUV).

A. Mission

The purpose of missions can be defined as visiting patrol locations as frequently as possible to detect undesirable situations earlier. This study defines the mission area as a

¹Kazuho Kobayashi is with Department of Mechanical Engineering, Materials Science, and Ocean Engineering, Graduate School of Engineering Science, Yokohama National University, Yokohama-city, Kanagawa, Japan kobayashi-kazuho-dj@ynu.jp or kazuho.kobayashi.ynu@gmail.com

²Seiya Ueno and Takehiro Higuchi with Faculty of Environment and Information Sciences, Yokohama National University {ueno-seiya-wk, higuchi}@ynu.ac.jp

This work has been submitted to the IEEE for possible publication. Copyright may be transferred without notice, after which this version may no longer be accessible.

two-dimensional grid map $G := \{g^k \mid k = 1, 2, \dots, K\}$. g^k denotes each grid corresponding to each patrol location, while K is the number of grids.

The parameter: *idleness* [8] i^k accompanies g^k as the elapsed time since any robot has last visited the grid. For instance, when a robot visited the grid g^k at time t^k and no other robot visited the grid since then, idleness at the current time t_c can be computed as $i^k(t_c) = t_c - t^k$. By this definition, one of the primary purposes of patrolling can be regarded as reducing idleness to maximize the chance of detecting undesired situations earlier. The study discretizes the time as integer values equal to or larger than zero.

B. Robots

A group of robots $R := \{r_n \mid n = 1, 2, \dots, N\}$ patrols the field where N is the number of robots. Each robot has capabilities to: (i)sense its accurate location \mathbf{x}_n , (ii)identify other robots and establish communication connection in its sensor range d_s , (iii)retain the connection once connected as long as the distance between the robots does not exceed the communication range d_c ($> d_s$). r_1 acts as the BS and is fixed at the origin of the map: $\mathbf{x}_1 = (0, 0)^T$ and does not participate in patrolling.

C. Performance metric

1) *Idleness*: To quantify the mission performance, this study introduces *graph idleness*: I_G and *worst idleness*: I_W as metrics. Based on the idleness $i^k(t)$ at each time instance, average graph idleness $I_G(t_c)$ at t_c can be computed as a mean value of i^k over all grids from the beginning of the mission $t = t_0$ until $t = t_c$:

$$I_G(t_c) = \frac{1}{(t_c - t_0 + 1)K} \sum_{t=t_0}^{t_c} \sum_{k=1}^K i^k(t) \quad (1)$$

Finally, I_G can be defined as $I_G := I_G(T)$, where T denotes the time at the end of the mission. Instantaneous worst idleness $I_W(t)$ denotes the largest value of i^k during $t_0 \leq t \leq t_c$:

$$I_W(t_c) = \max_{t_0 \leq t \leq t_c, k \in K} i^k(t) \quad (2)$$

and $I_W := I_W(T)$. I_G and I_W represent the general patrol performance and comprehensiveness of the patrol, respectively.

2) *Situation awareness*: This study also introduces mean SA delay D_{MSA} and worst SA delay D_{WSA} as performance metrics to quantify the SA of the BS. The definition follows the existing study [14]. In brief, the grid SA delay D_{SA}^k on a grid g^k can be computed as the difference between t_c and the last time instance t^k when the information on g^k is acquired (i.e., g^k is patrolled) as far as the BS is aware: $D_{SA}^k := t_c - t^k$. Due to the communication constraints, the BS cannot be aware immediately that g^k has been patrolled at t^k . When the information has not been delivered to the BS, D_{SA}^k is computed with the second latest t^k , or t^k is regarded as zero

when no robot has ever visited the grid. Instantaneous mean SA delay $D_{MSA}(t_c)$ is defined by:

$$D_{MSA}(t_c) = \frac{1}{(t_c - t_0 + 1)K} \sum_{t=t_0}^{t_c} \sum_{k=1}^K D_{SA}^k(t) \quad (3)$$

Finally, D_{MSA} is defined as $D_{MSA} := D_{MSA}(T)$. Similar to the worst idleness, instantaneous worst SA delay $D_{WSA}(t_c)$ can be computed by:

$$D_{WSA}(t_c) = \max_{t_0 \leq t \leq t_c, k \in K} D_{SA}^k(t) \quad (4)$$

and $D_{WSA} := D_{WSA}(T)$. These metrics show how late the BS acquires information on each grid. As described in the following section (Section III-A), t^k propagates among robots and reaches the BS. t^k grasped by the BS corresponds to the BS's assumption $t_{BS}^k \in h_{BS}^k$.

III. PROPOSED ALGORITHM

This section describes the proposed algorithm: LR. Each robot holds and updates its assumption about the map (Section III-A) and determines its patrol target (Section III-B).

A. Robotic assumption and its sharing

Since idleness is not measurable by external sensors of robots, each robot holds *assumed idleness* $H_n(t) := \{h_n^k(t) = [i_n^k(t), t_n^k(t)] \mid k \in K\}$ where $i_n^k(t)$ is assumed value of i^k by r_n at time t and $t_n^k(t)$ is the latest refresh time of $i_n^k(t)$. r_n increments its $i_n^k(t)$ as time passes based on the definition of idleness: $i_n^k(t) = i_n^k(t-1) + 1$ as if no other robots visit g^k . t_n^k keeps constant through this procedure since the growth of i_n^k is not confirmed by observation. When r_n has just visited g^k at t_c , it updates the assumption as: $i_n^k(t_c) \leftarrow 0$ and $t_n^k(t_c) \leftarrow t_c$ (i^k also becomes zero by its definition).

Each robot r_n also updates H_n every timestep when it is connected to other robots. The procedure is identical to [14]. In brief, r_n exchanges all $h_n^k \in H_n$ with $\forall r_m \in A_n$, while A_n is the group of robots directly connected to r_n . When t_n^k is smaller (i.e., the information is older) than t_m^k , r_n replaces h_n^k by h_m^k . Since h_n^k originally reflects r_n 's mission achievements, those achievements propagate through all other robots, including BS, as their shared knowledge.

B. Target selection

Each robot r_n determines its patrol target g_n^τ according to H_n and a parameter: ϵ_n , which denotes the degree of need to report to the BS. Algorithm 1 shows the process. In brief, r_n updates its assumption by the procedure in Section III-A (line 2) and also updates its ϵ_n (lines 3-4) according to the algorithm's operation mode described in the following subsections. Since the patrol progresses over time and the reporting need to the BS increases accordingly, ϵ_n grows over time in principle (line 3) while it is capped by ϵ_{max} . The function *update_epsilon* further updates ϵ_n to consolidate reporting needs to the BS to a single robot so that the other robots can continue patrolling free of the BS (line 4).

When r_n visits its current target, it selects a new patrol target grid g_n^τ after updating the assumption about the current

Algorithm 1 Target selection by r_n

```
1:  $H_n(t) \leftarrow H_n(t-1)$ 
2:  $H_n(t) \leftarrow \text{update\_assumption}(H_n(t))$ 
3: if connected to the BS then
4:    $\varepsilon_n \leftarrow 0$ 
5: end if
6:  $\varepsilon_n(t) \leftarrow \min\{\varepsilon_{max}, \varepsilon(t-1) + 1\}$ 
7:  $\varepsilon_n(t) \leftarrow \text{update\_epsilon}(r_n, mode)$ 
8: if  $r_n$  has just visited its current patrol target then
9:    $h_n^\tau \leftarrow [0, t]$ 
10:   $g_n^\tau \leftarrow \text{argmax}_{g^k \in G_n^\delta} U_n^k$ 
11:   $h_n^\tau \leftarrow [0, t]$ 
12: end if
```

target as *visited* (lines 5-7). The target candidates: G_n^δ are the local grids for r_n whose center is within distance δ from r_n . Finally, r_n selects g^k with the largest utility as g_n^τ according to the utility function (Equation 5). The utility of a grid g^k for r_n is first computed by $(i_n^k + \Delta_n^k) / \Delta_n^k$, while Δ_n^k is the expected travel time to g^k . After that, r_n boosts/reduces the utility of grids closer/farther to the BS, to increase the probability of moving towards the BS for reporting. r_n conversely reduces/boosts the utility of grids in order to patrol farther grids from the BS, when ε_n is small. E is a constant parameter to switch this process.

$$U_n^k = \begin{cases} (1 - \frac{\varepsilon_n - E}{\varepsilon_{max}}) * (\frac{i_n^k + \Delta_n^k}{\Delta_n^k}) & (\varepsilon_n \geq E, |\mathbf{x}^k| \geq |\mathbf{x}_n|) \\ (1 + \frac{\varepsilon_n - E}{\varepsilon_{max}}) * (\frac{i_n^k + \Delta_n^k}{\Delta_n^k}) & (\varepsilon_n \geq E, |\mathbf{x}^k| < |\mathbf{x}_n|) \\ (1 + \frac{E - \varepsilon_n}{\varepsilon_{max}}) * (\frac{i_n^k + \Delta_n^k}{\Delta_n^k}) & (\varepsilon_n < E, |\mathbf{x}^k| \geq |\mathbf{x}_n|) \\ (1 - \frac{E - \varepsilon_n}{\varepsilon_{max}}) * (\frac{i_n^k + \Delta_n^k}{\Delta_n^k}) & (\varepsilon_n < E, |\mathbf{x}^k| < |\mathbf{x}_n|) \end{cases} \quad (5)$$

To avoid target duplication with other robots, r_n preemptively updates the assumption for the selected grid (line 8). The value will be shared with the surrounding robots by *update_assumption* from the next time instance, informing other robots that the patrol need of this grid has been reduced.

The following two subsections describe the function *update_epsilon*(r_n , *mode*), which works based on the operation modes of the proposed algorithm.

1) *Operation mode A*: Mode A updates ε_n to transfer the value to a robot closer to the BS. Algorithm 2 shows the process. First, r_n compares distance from the BS to other robots $r_m \in A_n$. If r_n is the closest from the BS, it collects all ε_m with the discount rates η_1 and η_2 (line 2), and conversely is the farthest, it sets ε_n as zero (line 4). $|A_n|$ is the number

of robots in A_n . If neither is the case, then r_n collects ε_m of r_m which is farther from the BS than itself and has a certain amount of information to be reported (i.e., with larger ε_m than a certain threshold E_{th}) (lines 7-14). When there is no ε_m to collect (probably r_n has already collected ε_m before), r_n resets its ε_n as zero (lines 15-17). These procedures are expected to emerge role assignment: once a robot gets close to the BS, it keeps moving around the BS to collect the reporting needs of other robots (i.e., ε_n of other robots), and the other robots can patrol areas far from the BS.

Algorithm 2 *update_epsilon*(r_n , *mode* A)

```
1: if  $A_n \neq \emptyset$  then
2:   if  $\min(|\mathbf{x}_n|, \forall |\mathbf{x}_m| \in A_n) == |\mathbf{x}_n|$  then
3:      $\varepsilon_n \leftarrow \max(\varepsilon_n, \forall \varepsilon_m \in A_n) + \eta_1 \sum_m \varepsilon_m + \eta_2 |A_n|$ 
4:   else if  $\max(|\mathbf{x}_n|, \forall |\mathbf{x}_m| \in A_n) == |\mathbf{x}_n|$  then
5:      $\varepsilon_n \leftarrow 0$ 
6:   else
7:     is_transferred  $\leftarrow true$ 
8:     for all  $r_m \in A_n$  do
9:       if  $|\mathbf{x}_n| < |\mathbf{x}_m|$  &&  $\varepsilon_m > E_{th}$  then
10:         $\varepsilon_n \leftarrow \max(\varepsilon_n + \eta_1 \varepsilon_m, \varepsilon_m)$ 
11:        is_transferred  $\leftarrow false$ 
12:      end if
13:    end for
14:     $\varepsilon_n \leftarrow \varepsilon_n + \eta_2 |A_n|$ 
15:    if is_transferred == true then
16:       $\varepsilon_n \leftarrow 0$ 
17:    end if
18:  end if
19: end if
```

2) *Operation mode B*: Mode B makes a robot that has not communicated with the BS for a long time move towards the BS. The detailed process appears in Algorithm 3. r_n compares time instance t_n^{BS} when it last communicated with the BS to other robots $r_m \in A_n$. The process after that is similar to Algorithm 2, refreshing ε_n according to the result of the comparison. The mode is expected to provide robots with equal chances to communicate with the BS during the mission. These chances correspond to the opportunities of the system's check and battery re-charging at the BS in real-world applications.

IV. SIMULATIONS

A. Compared Algorithm

This study introduces several existing patrol algorithms for comparison. The adopted algorithms include one classic, high-performance algorithm and two latest algorithms. For comparison, the study modified the algorithms in the following points:

- Deploy one robot as a BS at the origin.
- Communication range is limited, as is the proposed algorithm.
- Robots hold assumed idleness and share with the BS when they are connected to compute D_{MSA} and D_{WSA} .

Algorithm 3 *update_epsilon(r_n, mode B)*

```
1: if  $A_n \neq \emptyset$  then
2:   if  $\min(t_n^{BS}, \forall t_m^{BS} \in A_n) == t_n^{BS}$  then
3:      $\epsilon_n \leftarrow \max(\epsilon_n, \forall \epsilon_m \in A_n) + \eta_1 \sum_m \epsilon_m + \eta_2 |A_n|$ 
4:   else if  $\max(t_n^{BS}, \forall t_m^{BS} \in A_n) == t_n^{BS}$  then
5:      $\epsilon_n \leftarrow 0$ 
6:   else
7:      $is\_transferred \leftarrow true$ 
8:     for all  $r_m \in A_n$  do
9:       if  $t_n^{BS} < t_m^{BS}$  &&  $\epsilon_m > E_{th}$  then
10:         $\epsilon_n \leftarrow \max(\epsilon_n + \eta_1 \epsilon_m, \epsilon_m)$ 
11:         $is\_transferred \leftarrow false$ 
12:       end if
13:     end for
14:      $\epsilon_n \leftarrow \epsilon_n + \eta_2 |A_n|$ 
15:     if  $is\_transferred == true$  then
16:        $\epsilon_n \leftarrow 0$ 
17:     end if
18:   end if
19: end if
```

Other limitations are described in each following subsection. The parameters of each algorithm were modified through preliminary simulations to adjust to the problem settings in this study. However, it is worth keeping in mind that the scope of this study does not include the optimization of the parameters for the existing algorithms; thus, the minor difference in the performance does not necessarily conclude the superiority of the algorithm in all situations. The following subsections describe the details of the algorithms.

1) *CR*: The Conscientious Reactive (CR) algorithm [8] makes each robot select the grid with the largest assumed idleness from grids adjacent to the robot as its patrol target. Though it is a classic algorithm, it is still comparable to many other algorithms, including centralized algorithms, at least in graph idleness.

2) *ER*: A robot implemented with Expected Reactive (ER) algorithm [11] computes the grid utility by its expected idleness to select the grid with the highest utility as its next target. Like CR, the target is selected from the adjacent grids to the robot. As for communications, ER restricts communications to share the arrival and the decision of targets. To be consistent with this restriction, the sharing of the assumed idleness described in Section III-A is also limited to the items about the arrived/selected target grids.

3) *DTAG*: The Dynamic Task Assignment Greedy algorithm (DTAG) [12] regards each patrol location as a task and assigns it to the robots according to its utility. Each robot computes the utility of all tasks in the field and selects the highest one as its task. DTAG allows robots to share their assumed idleness of all grids at every task assignment. Based on this characteristic, this study also allows robots to share the refresh time of those assumptions, as in Section III-A.

4) *DTAP*: The DTAP algorithm [12] is an advanced algorithm of DTAG. It adopts the market-based approach

to allocate tasks to the robots. Each robot evaluates a task utility at first, which is the same process as DTAG. Before engaging in the task, the robot computes its bid to the task and conducts an auction process with the neighbor robots. Finally, a robot with the lowest bid will be allocated the task. Other limitations and settings are the same as DTAG.

B. Configurations

Table I shows the configurations in the simulations. In each trial, N robots patrol the field with 600*600 [m] composed of 20 * 20 grids. At the beginning of each trial, the simulator deploys robot r_1 as the BS at the origin and deploys the others randomly in the fan-shaped area with $|x_n| < 2\sqrt{N}$ [m]. All values of idleness, assumed idleness, and update time of assumed idleness are initialized as zero. After the mission begins, each robot selects its patrol target grid according to the current patrol algorithm. Patrol of a grid is considered completed when a robot comes within three meters of the center of the target grid. All trials end at $T = 40000$ [sec], while seconds correspond to the simulation timestep in this study. The study conducted 5 trials for each condition: 90 trials in total (5 trials, 6 algorithms, 3 different N).

TABLE I
PARAMETERS AND CONFIGURATIONS

Symbol	Value	Unit	Comment
max_v_l	1.5	m/s	Max linear speed
max_v_a	1.0	rad/s	Max angular speed
d_c	180	m	Communication range
d_s	90	m	Sensor range
δ	180	m	Consider range for next target
ϵ_{max}	3000	-	-
E	500	-	-
N	4, 8, 12	robots	-
K	20 * 20	grids	-
-	30 * 30	m	grid size
T	40000	sec	duration of trial
-	5	-	# of trials per N per algorithm

C. Results

Figure 1 shows the screenshot of the simulation trial by: LR mode A (LR-A) with eight robots. In the figure, the color of the grids shows their idleness: the darker the color, the higher the idleness. The black circle at the left bottom denotes r_1 as the BS. Other robots are shown in cyan circles. The numbers appended to the robots except BS indicate ID in the upper row and ϵ_n in the lower row. The robots r_3 and r_4 are interconnected; thus, the value of ϵ_4 is kept to zero and aggregated to ϵ_3 of r_3 according to the function *update_epsilon* with mode A.

Table II overviews the results from the first of five trials conducted for each condition. In each column, the values with bold font show the smallest in the same N (the smaller is better by their definition, except for C_{SD}^B , which denotes the standard deviation of the number of connections with the BS). Figure 2 and Figure 3 further visualize the results of the same trials. The symbol 'x' denotes the mean value in each box, corresponding to I_G and D_{MSA} , respectively. The largest

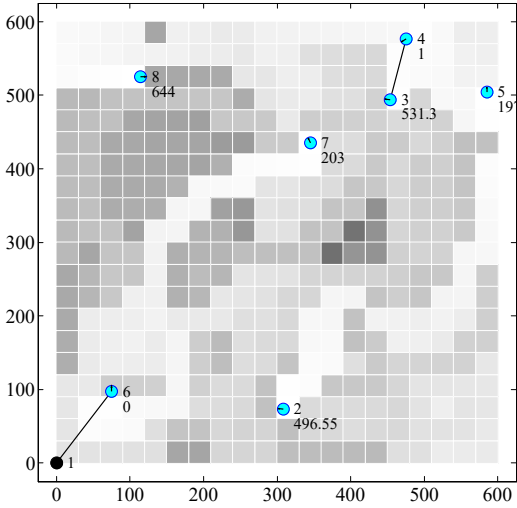


Fig. 1. Screenshot of the simulated patrol mission by the proposed algorithm ($N = 8$). The black circle, cyan circles, and lines denotes the BS, robots, and connections. The color of grids corresponds to the ground truth of their idleness, the darker the color, the higher the idleness.

values of each box correspond to I_W and D_{WSA} . Several values do not appear in the figures but only in Table II since the vertical axes are expanded. To eliminate the effect of transition phase at the beginning of missions, all results show the data during $20001 \leq t \leq 40000$, except for C_{SD}^B .

TABLE II

SIMULATION RESULTS OF THE FIRST OF FIVE TRIALS CONDUCTED FOR EACH CONDITION

N	Algorithm	I_G	I_{SD}	I_W	D_{MSA}	D_{WSA}	C_{SD}^B
4	CR	3387	2692	20424	9299	31221	0.47
	ER	2286	1850	12159	4851	20194	1.70
	DTAG	2720	1712	8658	4944	13287	1.25
	DTAP	2909	1879	9304	5270	14861	0.47
	*LR-A	2092	1521	10246	2848	11263	1.70
	*LR-B	2180	1692	13980	2970	14900	0.47
8	CR	1569	1338	8640	4647	16530	1.91
	ER	1121	960	6824	3006	11258	1.58
	DTAG	1143	806	4773	2513	7200	1.51
	DTAP	1143	796	4405	2597	7979	1.76
	*LR-A	850	622	4200	1337	5139	2.33
	*LR-B	819	580	4158	1327	4810	0.76
12	CR	1098	1006	7445	4062	13896	1.23
	ER	698	622	4760	2309	9764	1.00
	DTAG	692	516	3596	1684	7122	1.66
	DTAP	692	494	3320	1511	5326	2.17
	*LR-A	535	397	2751	906	3521	2.90
	*LR-B	533	395	3013	980	3371	0.62

* denotes the proposed algorithms in this study.
All values were collected during $20001 \leq t \leq 40000$.

In Table II and Figure 2 and 3, the lower I_G by LR indicates that the robots patrolled each location more frequently, corresponding to the higher chance of detecting undesired situations earlier in real-world applications. Furthermore, the lower I_{SD} and I_W result from balanced and comprehensive patrol, not leaving a certain grid unpatrolled for long. This perspective is also important to avoid the worst case: leaving

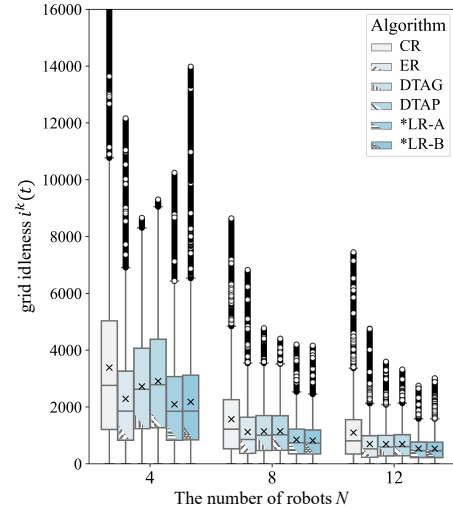


Fig. 2. Box plot for all grid idleness: $I^k(t)$ during $20001 \leq t \leq 40000$ in the first of five trials conducted for each condition. The vertical axis is expanded, and values larger than 16000 do not appear. * in the legend denote that those are the proposed algorithms.

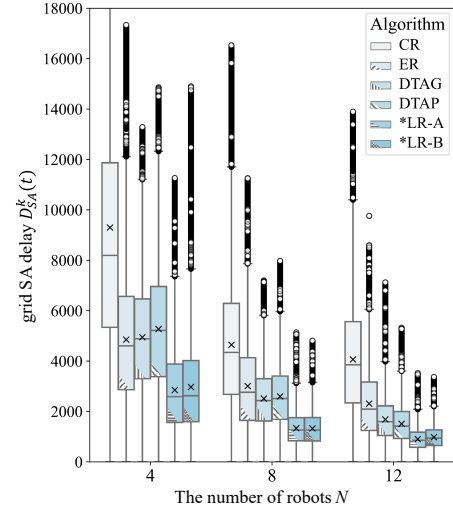


Fig. 3. Box plot for all grid SA delay of the BS: $D_{SA}^k(t)$ during $20001 \leq t \leq 40000$ in the first of five trials conducted for each condition. The vertical axis is expanded and values larger than 18000 do not appear. * in the legend denote that those are the proposed algorithms.

the undesired situation for a long time, and humans cannot be aware of the situation. LR also performed well in these metrics, though they were the third and fourth best in I_W when $N = 4$ (Table II). DTAG and DTAP performed comparably to LR in I_W since they consider all grids at target selection and can detect high idleness grids earlier. The larger consider range δ , like these algorithms, may improve LR performance in I_W . Figure 4 and Figure 5 further show I_G and I_W of all five trials. The figures show that the result in Table II were consistently demonstrated in all trials.

The performance of LR in SA was also superior, as shown in Table II, Figure 2, and Figure 3. Though D_{WSA} in some cases were worse due to the worse I_W , most performance by LR, especially in D_{MSA} , was better than the others.

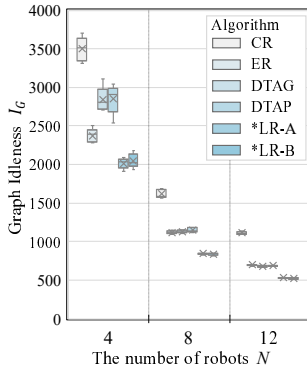


Fig. 4. Box plot of Graph Idleness: I_G by all five trials

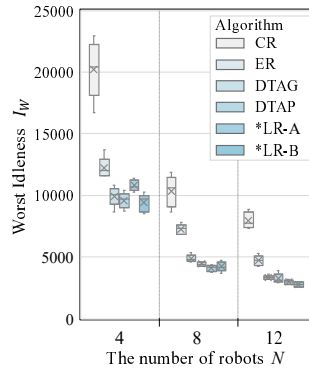


Fig. 5. Box plot of Worst Idleness: I_W by all five trials

These metrics show how well the BS is informed about the grids, and the lower metrics indicate the BS grasps the grid information with less delay, which leads to better SA. These metrics correspond to the elapsed time since information, such as captured images, collected specimens, and picked-up objects, is acquired as far as the BS is aware. Figure 6 and Figure 7 further demonstrate these results by plotting the data of all five trials. All trials showed the same trend as Table II that LR performed better in the aspect of SA.

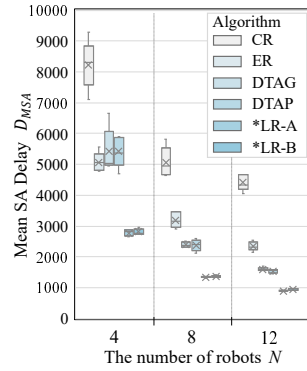


Fig. 6. Box plot of Mean SA delay: D_{MSA} by all five trials

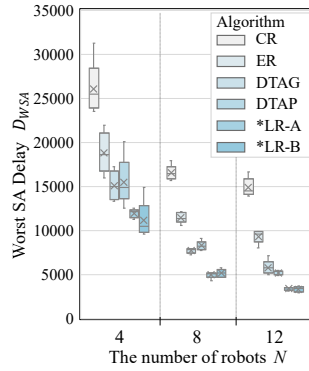


Fig. 7. Box plot of Worst SA delay: D_{WSA} by all five trials

The performance of LR-A and LR-B is almost identical, while the major difference appears in C_{SD}^B , which indicates the standard deviation of the number of times robots have connected to the BS. LR-A showed consistently higher C_{SD}^B in all N . This indicates that the algorithm showed the emergent role allocation: some robots take a role to move around the BS, to collect and report the other robots' achievements, while other robots take another role to patrol the farther area to the BS. On the other hand, LR-B showed a smaller value in C_{SD}^B in all N , indicating the almost equal number of times the robots connect to the BS. These trends are well consistent with the design intent of the two operation modes.

Though the existing algorithms performed poorly in most metrics, the result alone does not mean they perform poorly in all situations. One of the possible reasons other than parameter optimization is that these algorithms are not designed for the grid map but for the topological graphed map, which

is suitable to represent environments such as indoor fields with corridors and rooms. In this study, LR performed well with frequent communication for accurate assumptions about grids' idleness and appropriate consideration range for target selections. These characteristics may be suitable for a grid map with a larger number of grids and fewer restrictions to path selection than graphed maps. Future works will study the effect of environmental representation, robot failures, and communication latency, as well as real-world experiments.

V. CONCLUSION

This study proposed an algorithm for multi-robot patrolling conscious for the situation awareness of the base stations. The algorithm is distributed and works according to individual robots' perceptions and communications with nearby robots. The proposed algorithm performed better than the existing algorithms, in most metrics for patrolling and the base station's situation awareness.

REFERENCES

- [1] M. Schranz, M. Umlauf, M. Sende, and W. Elmenreich, "Swarm Robotic Behaviors and Current Applications," *Frontiers in Robotics and AI*, vol. 7, no. 36, 2020.
- [2] D. Carrillo-Zapata, E. Milner, J. Hird, G. Tzoumas, P. J. Vardanega, M. Sooriyabandara, M. Giuliani, A. F. Winfield, and S. Hauert, "Mutual Shaping in Swarm Robotics: User Studies in Fire and Rescue, Storage Organization, and Bridge Inspection," *Frontiers in Robotics and AI*, vol. 7, no. 53, apr 2020.
- [3] N. R. Gans and J. G. Rogers, "Cooperative Multirobot Systems for Military Applications," *Current Robotics Reports*, vol. 2, no. 1, pp. 105–111, 2021.
- [4] M. R. Endsley, "Design and Evaluation for Situation Awareness Enhancement," *Proceedings of the Human Factors Society Annual Meeting*, vol. 32, no. 2, pp. 97–101, oct 1988.
- [5] J. Banfi, N. Basilico, and F. Amigoni, "Minimizing communication latency in multirobot situation-aware patrolling," in *2015 IEEE/RSJ International Conference on Intelligent Robots and Systems (IROS)*, 2015, pp. 616–622.
- [6] J. Scherer and B. Rinner, "Multi-Robot Patrolling with Sensing Idleness and Data Delay Objectives," *Journal of Intelligent and Robotic Systems*, vol. 99, no. 3, pp. 949–967, 2020.
- [7] L. Huang, M. Zhou, K. Hao, and E. Hou, "A survey of multi-robot regular and adversarial patrolling," *IEEE/CAA Journal of Automatica Sinica*, vol. 6, no. 4, pp. 894–903, 2019.
- [8] A. Machado, G. Ramalho, J.-D. Zucker, and A. Drogoul, "Multi-agent Patrolling: An Empirical Analysis of Alternative Architectures," in *Multi-Agent-Based Simulation II*, 2003, pp. 155–170.
- [9] D. Portugal and R. P. Rocha, "Distributed multi-robot patrol: A scalable and fault-tolerant framework," *Robotics and Autonomous Systems*, vol. 61, no. 12, pp. 1572–1587, 2013.
- [10] D. Portugal, M. S. Couceiro, and R. P. Rocha, "Applying Bayesian learning to multi-robot patrol," in *2013 IEEE International Symposium on Safety, Security, and Rescue Robotics (SSRR)*, 2013, pp. 1–6.
- [11] C. Yan and T. Zhang, "Multi-robot patrol: A distributed algorithm based on expected idleness," *International Journal of Advanced Robotic Systems*, vol. 13, no. 6, pp. 1–12, nov 2016.
- [12] A. Farinelli, L. Iocchi, and D. Nardi, "Distributed on-line dynamic task assignment for multi-robot patrolling," *Autonomous Robots*, vol. 41, no. 6, pp. 1321–1345, 2017.
- [13] J. Banfi, A. Quattrini Li, I. Rekleitis, F. Amigoni, and N. Basilico, "Strategies for coordinated multirobot exploration with recurrent connectivity constraints," *Autonomous Robots*, vol. 42, no. 4, pp. 875–894, 2018.
- [14] K. Kobayashi, T. Higuchi, and S. Ueno, "Hierarchical and Distributed Patrol Strategy for Robotic Swarms with Continuous Connectivity," in *Proceedings of the Joint Symposium of AROB-ISBC-SWARM2023*, 2023, pp. 1491–1496.